AWARD NUMBER: W81XWH-20-1-0093

TITLE:
Targeting 3beta-HSD1 phosphorylation to reverse prostate cancer hormone therapy resistance

PRINCIPAL INVESTIGATOR:
Xiuxiu Li

CONTRACTING ORGANIZATION:
Cleveland Clinic Foundation, Cleveland, OH

REPORT DATE:
January 2023

TYPE OF REPORT:
Final

PREPARED FOR: U.S. Army Medical Research and Development Command
Fort Detrick, Maryland 21702-5012

REPORT DOCUMENTATION PAGE

Form Approved
OMB No. 0704-0188

1. REPORT DATE	**2. REPORT TYPE**	**3. DATES COVERED**
January 2023	Final	30Sep2020-29Sep2022

4. TITLE AND SUBTITLE

Targeting 3beta-HSD1 phosphorylation to reverse prostate cancer hormone therapy resistance

5a. CONTRACT NUMBER
W81XWH-20-1-0093

5b. GRANT NUMBER
GRANT12890068

5c. PROGRAM ELEMENT NUMBER
PC190587

6. AUTHOR(S)
Xiuxiu Li

E-Mail: lix7@ccf.org

5d. PROJECT NUMBER

5e. TASK NUMBER

5f. WORK UNIT NUMBER

7. PERFORMING ORGANIZATION NAME(S) AND ADDRESS(ES)
Cancer Biology, Lerner Research Institute
Cleveland Clinic Foundation
9500 Euclid AVE
Cleveland, OH, 44195

8. PERFORMING ORGANIZATION REPORT NUMBER

9. SPONSORING / MONITORING AGENCY NAME(S) AND ADDRESS(ES)
U.S. Army Medical Research and Development Command
Fort Detrick, Maryland 21702-5012

10. SPONSOR/MONITOR'S ACRONYM(S)

11. SPONSOR/MONITOR'S REPORT NUMBER(S)

12. DISTRIBUTION / AVAILABILITY STATEMENT
Approved for Public Release; Distribution Unlimited

13. SUPPLEMENTARY NOTES

14. ABSTRACT

Prostate cancer is the most common malignancy in men and the second leading cause of cancer-related death in men in the United States. Androgen deprivation therapy (ADT) is the front-line treatment, but it eventually fails and disease almost always progresses as castration-resistant prostate cancer (CRPC). Nearly all prostate cancer deaths are due to CRPC. It has been demonstrated that intratumoral androgen synthesis is required to drive CRPC progression. The enzyme 3β-hydroxysteroid dehydrogenase type 1 (3βHSD1), which catalyzes the initial rate-limiting step in the conversion of the adrenal-derived steroid dehydroepiandrosterone to dihydrotestosterone (the most potent natural stimulus of the androgen receptor), is likely a critical enzymatic gatekeeper that confers on tumors the ability to harness adrenal androgens. Genetic evidence in men demonstrates the role of 3βHSD1 in driving CRPC. In postmenopausal women, 3βHSD1 is required for synthesis of aromatase substrates and plays an essential role in breast cancer. Therefore, 3βHSD1 lies at the major decision point for synthesis of androgens vs. estrogens and where metabolic flux is also genetically regulated through germline inheritance. I have found that phosphorylation of Y344 occurs, is required for 3βHSD1 cellular activity and generation of Δ4, 3-keto-substrates of 5α-reductase and aromatase, including in patient tissues. I also demonstrated BMX directly interacts with 3βHSD1 and is necessary for enzyme phosphorylation and androgen biosynthesis. *In vivo* investigation showed that blockade of 3βHSD1 Y344 phosphorylation inhibits CRPC. These findings identify new hormonal therapy pharmacologic vulnerabilities for sex-steroid dependent cancers.

15. SUBJECT TERMS
3βHSD1, phosphorylation, BMX, DHEA metabolism, CRPC

16. SECURITY CLASSIFICATION OF:			**17. LIMITATION OF ABSTRACT**	**18. NUMBER OF PAGES**	**19a. NAME OF RESPONSIBLE PERSON**
a. REPORT	**b. ABSTRACT**	**c. THIS PAGE**			USAMRDC
Unclassified	Unclassified	Unclassified	Unclassified	23	**19b. TELEPHONE NUMBER** *(include area code)*

Table of Contents

	Page
1. Introduction……	4
2. Keywords……	4
3. Accomplishments……..……..…….	5-14
4. Impact……..…….	15
5. Changes/Problems...…….	15
6. Products……..……..……	16
7. Participants & Other Collaborating Organizations……..	16
8. Special Reporting Requirements…….	17
9. Appendices…….	18-23

INTRODUCTION:

PCa is the most common malignancy in men and the second leading cause of cancer-related death in men in the United States. Prostate cancer progression depends on continued androgen receptor (AR) activity. Testosterone and its more potent metabolite, 5α-dihydrotestosterone (DHT), are the endogenous ligands that activate the AR in health, and in PCa they are the ligands fueling the growth of malignant prostate cells. Androgen deprivation therapy (ADT), either by medical or surgical castration, is the front-line treatment, but it almost always eventually progresses as castration-resistant prostate cancer (CRPC). The Sharifi laboratory has demonstrated that intratumoral androgen synthesis is required for driving CRPC progression. Intratumoral synthesis of DHT from precursors that are secreted from the adrenal gland occurs through a pathway that circumvents testosterone. This synthesis requires three enzymes: 3β-hydroxysteroid dehydrogenase (3βHSD; encoded by HSD3B), steroid-5α-reductase (SRD5A), and the 17β-hydroxy steroid dehydrogenase (17βHSD) isoenzymes. 3β-hydroxysteroid dehydrogenase type 1 (3βHSD1), which catalyzes the initial rate-limiting step in the conversion of the adrenal-derived steroid dehydroepiandrosterone (DHEA) to DHT, is a critical enzymatic gatekeeper that confers on tumors the ability to harness adrenal androgens. A *HSD3B1*(1245A>C) variant has been mechanistically linked to CRPC by encoding an altered enzyme that augments DHT synthesis. Inheritance of the *HSD3B1* allele that enhances DHT synthesis is associated with prostate cancer resistance to ADT. Also, it has been reported that the *HSD3B1* variant regulates dueling abiraterone metabolite effects in prostate cancer. Recently we identified and genotyped 475 Caucasian men enrolled in the CHAARTED trial, which evaluated the ability of early chemotherapy to improve overall survival of patients starting ADT for metastatic prostate cancer, and found that inheritance of the *HSD3B1*(1245C) allele that augments DHT synthesis from adrenal precursors may be associated with more rapid development of CRPC and lower overall survival in Caucasian men with low-volume metastatic prostate cancer treated with ADT with or without docetaxel.

Protein phosphorylation is a reversible post-translational modification of proteins in which protein kinase phosphorylates an amino acid residue by adding a covalently bound phosphate group. Phosphorylation alters the structural conformation of a protein, causing it to become activated, deactivated, or otherwise modifying its function. 3βHSD1 is critical to androgen synthesis and prostate cancer growth, but no functional phosphorylation sites have been reported. Epithelial and endothelial tyrosine kinase (Etk, also known as BMX) is a non-receptor tyrosine kinase that has been implicated in various biological processes, including proliferation, differentiation, apoptosis, and cell migration. BMX expression is up-regulated in response to androgen ablation in prostate cancer, suggesting that Etk/BMX may be involved in the development and progression of CRPC. However, the downstream mechanisms of BMX action remain elusive, and it has no known role in regulating androgen synthesis. I have identified multiple phosphorylation sites on 3βHSD1 and found that phosphorylation of a single tyrosine (Y) is required for 3βHSD1 activation and that BMX is the necessary kinase. I also demonstrated BMX blockade inhibits metabolism of (Δ5, 3β-OH) DHEA to (Δ4, 3-keto) Δ4-androstenedione (AD), which is the major substrate for steroid-5α-reductase (SRD5A) and aromatase, downstream enzymes required for potent androgen and estrogen synthesis, respectively. Next, I found that BMX therefore regulates the generation of the Δ4, 3-keto-steroid structure, which is necessary for all potent sex steroids. Finally, I discovered that targeting BMX is a potential treatment strategy for CRPC.

KEYWORDS:

3βHSD1, phosphorylation, BMX, DHEA metabolism, CRPC

ACCOMPLISHMENTS:

What were the major goals of the project?

Training-Specific Tasks:

Milestone(s) Achieved: Completion of Research Conduct and Human Subjects Training

Milestone(s) Achieved: Attend monthly Prostate Cancer Working Group & Seminar Series
Milestone(s) Achieved: Attend and present research at weekly lab meetings and journal clubs

Milestone(s) Achieved: Attend and present research at Cleveland Clinic Department of Cancer Biology seminars

Milestone(s) Achieved: Attend 2 national meetings -- not yet. Have submitted abstract for presentation at AACR 2023

Research-Specific Tasks:

Specific Aim 1: Confirm that phosphorylation of 3βHSD1 indeed modifies its function and plays a role in prostate cancer cell growth.

Major Task 1: Identify the functional phosphorylation sites on 3βHSD1 (6 months).

Milestone(s) Achieved: Identification of the functional phosphorylation sites on 3βHSD1. (6 months)

Major Task 2: Determine whether phosphorylation of 3βHSD1 affects prostate cancer cell growth (11 months).

Milestone(s) Achieved: Determination that phosphorylation of 3βHSD1 at functional site is required for prostate cancer cell growth (11 months).

Major Task 3: Determine whether phosphorylation of 3βHSD1 is increased or decreased in patients with prostate cancer (16 months).

Milestone(s) Achieved: See "Other Achievement 6, Effects of BMX inhibition on 3βHSD1 phosphorylation and androgen synthesis in fresh human prostate tissues."

Specific Aim 2: Determine the effect of AMPK on androgen synthesis and prostate cancer cell growth, and identify the mechanism.

Major Task 4: Determine the mechanism by which AMPK regulates 3βHSD1 activity (18 months).

Milestone(s) Achieved: Not yet.

Major Task 5: Determine whether sh-AMPK or the AMPK inhibitor, Compound C, affects prostate cancer cell growth (21 months).

Milestone(s) Achieved: Not yet.

Major Task 6: Analyze AMPK expression in tumor tissue from prostate cancer patients and the correlation of AMPK with patient survival (24 months).

Milestone(s) Achieved: Not yet.

What was accomplished under these goals?

Accomplished tasks:

Specific Aim 1: Confirm that phosphorylation of 3βHSD1 indeed modifies its function and plays a role in prostate cancer cell growth.

Major Task 1: Identify the functional phosphorylation sites on 3βHSD1 (6 months).

Milestone(s) Achieved: Identification of the functional phosphorylation sites on 3βHSD1 (6 months).

Results:

To test whether phosphorylation is necessary for 3βHSD1 activity, we overexpressed HA-3βHSD1 in C4-2 cells. Immunoblotting analyses of immunoprecipitated HA-3βHSD1 with anti-phospho-tyrosine antibodies showed that 3βHSD1 undergoes tyrosine phosphorylation, which is induced in the presence of its substrates DHEA, pregnenolone, and androstenediol **(Fig. 1A)**. Mass spectrometry analyses of immunoprecipitated GST-3βHSD1 expressed in C4-2 cells showed that 3βHSD1 was phosphorylated at tyrosine (Y) 255 and tyrosine (Y) 344 **(Fig. 1B and Fig. S1, C to D)**. This result was further supported by immunoblotting analyses. Mutation of Y344 or Y255 to phenylalanine reduced tyrosine phosphorylation of 3βHSD1 **(Fig. 1C)**. Further, I found that phosphorylation of Y344 but not Y255 is required for 3βHSD1 cellular activity because DHEA metabolism was significantly reduced after mutation to phenylalanine **(Fig. 1D and Fig. S1E)**. To gain further insight about the mechanisms of this modification, we custom-designed an anti-phospho-3βHSD1 Y344 (anti-3βHSD1 pY344) antibody. After determining that it had excellent specificity **(Fig. S1F)**, I used it to detect 3βHSD1 pY344 in C4-2 and LNCaP cells. We found that 3βHSD1 pY344 was induced by DHEA treatment **(Fig. 1E)**. Collectively, these results indicate that Y344 phosphorylation is essential for 3βHSD1 enzyme activity in cells.

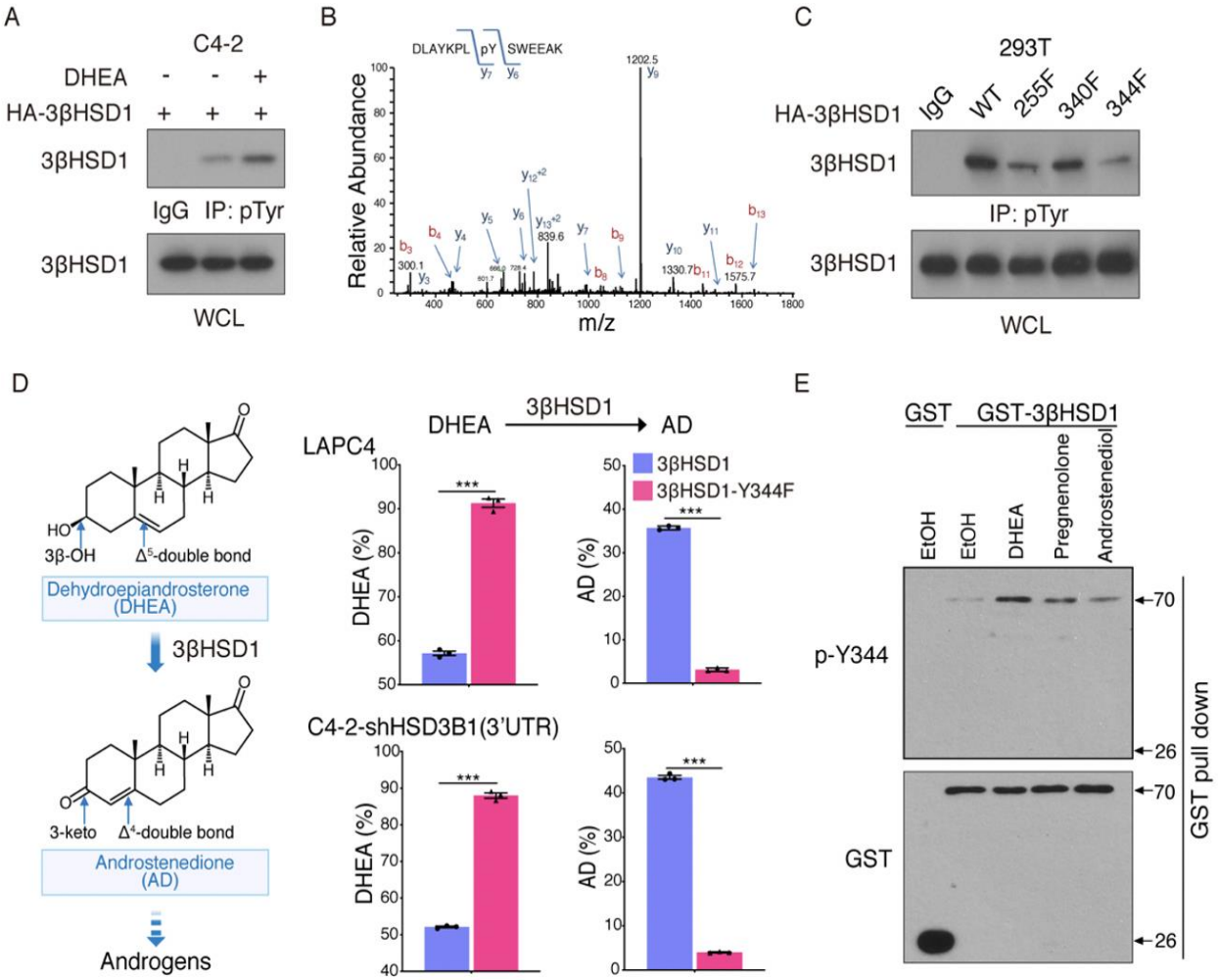

Fig 1. 3β-hydroxysteroid dehydrogenase (3βHSD1) pY344 is required for DHEA metabolism. A. C4-2 cells overexpressing HA-3βHSD1 were treated with or without DHEA for 1 hour. Pan-phospho-tyrosine (pTyr) was detected by immunoprecipitation and western blot. Control lysate without DHEA treatment was used for the IgG control. **B.** 3βHSD1-GST was transfected, and cells were treated with DHEA for 1 hour. GST pull-down complexes were immunoblotted, and the indicated phosphopeptides on human 3βHSD1 were identified by LC-MS/MS. A doubly charged peptide with a mass of 896.91 Da was identified in the survey analysis of GST-HSD3B1. The CID spectra for this peptide are dominated by singly charged C-terminal y ions. The mass difference between y_7 and y_6 is consistent with modification at Y344. **C.** Cells were transfected with HA-3βHSD1 mutants and treated as in (A). Lysate from WT-expressing cells was used for the IgG control. **D.** 3βHSD1 enzyme activity was assessed by analyzing DHEA metabolism by HPLC. Cells were transfected with Flag-3βHSD1 mutants and subsequently treated with [^{3}H]-DHEA for 4 hours, followed by steroid extraction from media, steroid separation, and quantitation with HPLC. The experiment was done in triplicate and

repeated in independent experiments. Shown are the steroid sites of 3βHSD1 biochemical modification. Mean ± SEM represents 3 replicates in 1 experiment. Three independent experiments were performed. ***P < 0.001 (unpaired 2-tailed t-test). **E.** C4-2 cells overexpressing 3βHSD1-GST were treated with ethanol or DHEA, pregnenolone, or androstenediol for 1 hour. GST pull-down complexes were immunoblotted with a phospho-3βHSD1-Y344 antibody.

Major Task 2: Determine whether phosphorylation of 3βHSD1 affects prostate cancer cell growth (11 months).

Milestone(s) Achieved: determination that phosphorylation of 3βHSD1 at functional site is required by prostate cancer cell growth (11 months).

Results:

To determine whether phosphorylation of 3βHSD1 affects prostate cancer cell growth, I produced C4-2 cell lines that stably expressed 3βHSD1 (WT) or 3βHSD1-Y344F. DHEA metabolism was retarded in the 3βHSD1-Y344F cell line **(Fig. 4A)**. I then tested cell viability and proliferation using the WST-1 assay and found that the Y344F mutation of 3βHSD1 inhibits DHEA-stimulated cell proliferation **(Fig. 4B)**. Further, the 3βHSD1 Y344F mutation inhibited AR-dependent transcriptional activity of canonical AR-regulated genes **(Fig. 4C)**. Our results suggest that 3βHSD1 pY344 phosphorylation promotes prostate cancer cell progression.

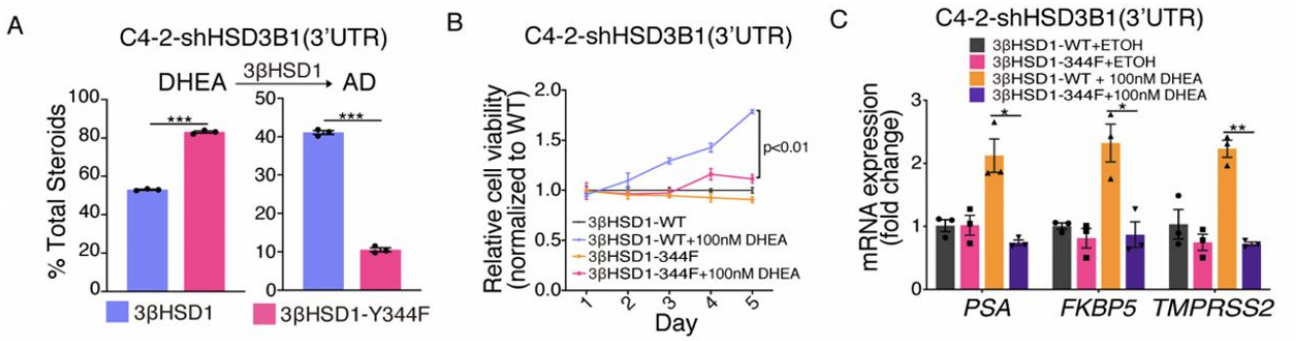

Fig 4. BMX blockade and inhibition of 3βHSD1 phosphorylation inhibit expression of androgen-regulated genes and prostate cancer proliferation. A. C4-2 cells with stable shRNA-mediated knockdown of 3βHSD1 were stably infected with lentivirus expressing either 3βHSD1 (WT) or 3βHSD1-Y344F and subsequently treated with [^{3}H]-DHEA for 5 hours, followed by steroid extraction from media and steroid separation and quantitation with HPLC. **B.** As in (A), but cells were deprived of serum overnight, followed by treatment with DHEA for the indicated days; cell proliferation was assessed with the WST-1 assay and growth for each cell line was normalized to WT control for each designated day. **C.** As in (A), but cells were deprived of serum overnight and treated with DHEA for 48 hours, followed by RNA extraction and qPCR. Expression is normalized to control and *RPLP0* expression.

I next sought to determine the requirement for 3βHSD1 pY344 phosphorylation in development of CRPC *in vivo* in mouse xenograft models. We generated C4-2 cell lines that stably expressed 3βHSD1 (WT) or 3βHSD1-Y344F, subcutaneously injected the cells into male NSG mice to generate tumors, followed by surgical castration and subcutaneous implantation of 90-day sustained-release DHEA pellets to mimic the human physiology that occurs with ADT and CRPC development, similar to our prior studies (mice do not produce DHEA). We found that the Y344F mutation of 3βHSD1 inhibited DHEA-induced tumor growth and prolonged progression-free survival in C4-2 xenograft models of CRPC **(Fig. 5, A and B)**. Mass spectrometry assessment of androgens in xenograft tissues **(Fig. 5C)** demonstrated that the Y344F mutation inhibited tumor growth through loss of intratumoral androgen production. Reduction in AR transcriptional activity also was detected in xenograft tumors carrying mutated Y344F **(Fig. 5D)**. In contrast, the Y344F mutation had no significant effect on tumor growth, progression-free survival, tissue testosterone, and androgen signaling in xenografts growing in eugonadal mice **(Fig. S5, A-D)**.

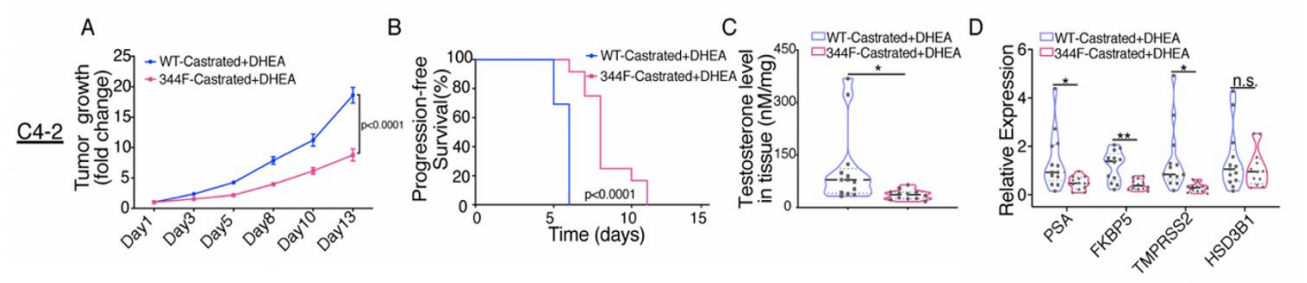

Fig 5. 3βHSD1-Y344F BMX pharmacologic blockade and 3βHSD1-Y344F inhibit androgen biosynthesis and CRPC growth in vivo. A. C4-2 cells with stable shRNA-mediated knockdown of 3βHSD1 were stably infected with a lentivirus expressing 3βHSD1 (WT) or 3βHSD1-Y344F. Mice were subcutaneously injected with 10 million cells, and castration plus DHEA pellet implantation were performed after tumors reached 200 mm^3. Tumor growth is shown as fold change from the time of treatment initiation for each tumor. The numbers of mice in the WT-3βHSD1/castration and 344F-3βHSD1/castration groups were 13 and 12, respectively. **B.** Progression-free survival was assessed as time to 3-fold increase in tumor volume from treatment initiation. **C.** The testosterone concentration in xenograft tumors was detected by mass spectrometry. **D.** RNA was extracted from xenograft tumors, expression of AR responsive genes (*PSA*, *FKBP5* and *TMPRSS2*) and *HSD3B1* was determined by qPCR. Expression is normalized to control and *RPLP*0 expression.

Other achievements:

Because the phosphorylation site we found was tyrosine phosphorylation site, so next in the study of kinase, we decided to continue to pursue regulatory tyrosine kinase. Therefore, as I reported in my *JCI* paper, I investigated the tyrosine kinase that phosphorylates 3βHSD1 at Y344 and the underlying mechanism.

Other Achievement 1: BMX is required for DHEA metabolism by 3βHSD1.

To identify the kinase that phosphorylates 3βHSD1, we used a kinase inhibitor library to screen in an unbiased fashion for pharmacologic inhibitors that block [3H]-DHEA metabolism **(Fig. S2A)**. HPLC analyses showed that pharmacologic inhibitors of BMX or PDGFR block [3H]-DHEA metabolism to (Δ4, 3-keto) Δ4-androstenedione (AD). Kinase prediction based on Y344 using the phosphoNET Kinase Predictor (http://www.phosphonet.ca/kinasepredictor.aspx?uni=P14060&ps=Y344) showed that BMX had the greatest potential to phosphorylate 3βHSD1 at Y344. Further, we tested several BTK/BMX inhibitors, with HPLC analyses showing that zanubrutinib or ibrutinib treatment significantly decreased DHEA metabolism in multiple prostate cancer (LNCaP, C4-2 and VCaP) cell lines **(Fig. 2A and Fig. S2, B to D)**. The 3β-OH → 3-keto and Δ5 → Δ4 reactions catalyzed by 3βHSD1 to synthesize AD do not only serve to make this a substrate of steroid-5α-reductase (SRD5A) -- these reactions are also essential to generate 3-keto, Δ4-steroid substrates (e.g., AD and testosterone) for aromatase and estrogen biosynthesis. Thus, we examined the effect of BMX inhibition on estrogen synthesis from DHEA as a precursor. We found that zanubrutinib also inhibits the production of estradiol from DHEA **(Fig. S2E)**.

We generated LNCaP cells stably expressing shNT (non-targeting control) or shRNA sequences against BMX (shBMX) and found that knocking down BMX also inhibited DHEA metabolism (**Fig. 2B**). We next examined the interaction between 3βHSD1 and BMX. Co-immunoprecipitation assays showed that 3βHSD1 interacted with BMX (**Fig. 2, C and D**), and this interaction was induced by the 3βHSD1 substrates DHEA, pregnenolone, and androstenediol (**Fig. 2E**). Moreover, we found that 3βHSD1 substrates induced (**Fig. 2F**) and are required for the phosphorylation of BMX (**Fig. 2G**). In the absence of 3βHSD1, DHEA failed to activate the phosphorylation of BMX, suggesting that DHEA-mediated 3βHSD1-BMX interaction is needed for BMX activation. Taken together, our findings indicate that BMX is required for DHEA metabolism by 3βHSD1.

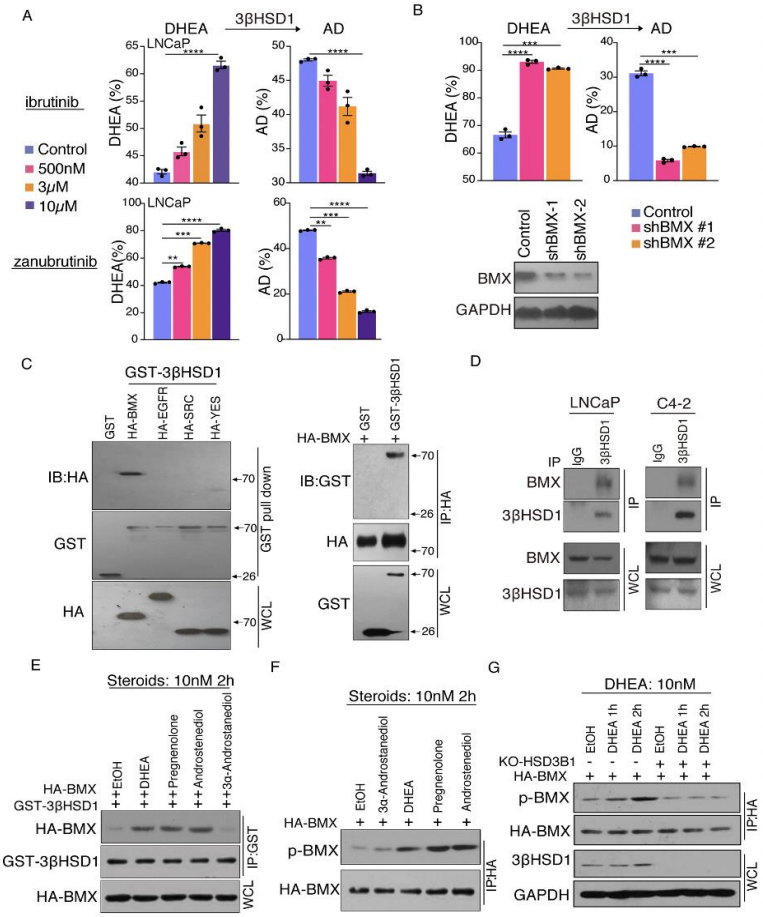

Fig 2. BMX is required for DHEA metabolism by 3βHSD1. A. LNCaP cells were treated with ibrutinib or zanubrutinib for 1 hour and subsequently treated with [^{3}H]-DHEA for 5 hours, followed by steroid extraction from media and steroid separation and quantitation with HPLC. The experiment was done in triplicate and repeated in independent experiments. Mean ± SEM represents 3 replicates in 1 experiment. Three independent experiments were performed. **P < 0.01, *** P < 0.001, **** P < 0.0001 (1-way ANOVA test with Dunnett's multiple comparisons test). **B.** Cells stably expressing shNT or two shRNA sequences against BMX were treated with [^{3}H]-DHEA for 6 hours and analyzed as in (A). Mean ± SEM represents combined data from 3 biological independent replicates performed in technical triplicate. *** P < 0.001, **** P < 0.0001 (1-way ANOVA test with Dunnett's multiple comparisons test). **C.** 293T cells were transiently co-transfected with HA-BMX, EGFR, SRC, or YES and GST-3βHSD1, followed by GST pull-down and western blot (left). 293T cells were transiently co-transfected with HA-BMX and GST-3βHSD1, followed by HA immunoprecipitation and western blot (right). **D.** LNCaP and C4-2 cells were cultured, protein collected, and immunoprecipitation and western blot performed for endogenously expressed proteins. WCL blots run in parallel, contemporaneously, using identical samples are shown. **E.** LNCaP cells were transiently co-transfected with HA-BMX, and GST-3βHSD1cells were starved with medium containing 10% charcoal-stripped fetal bovine serum for 24 hours, then treated with steroids for 2 hours, followed by GST-pull down and western blot to detect interaction of HA-BMX and GST-3βHSD1. **F.** LNCaP cells were starved as in (E), then transfected with HA-BMX and treated with steroids for 2 hours; p-BMX was detected by western blot. Blots run in parallel, contemporaneously, using identical samples are shown. **G.** Stable C4-2 cell lines with *HSD3B1* gRNA or control gRNA were transfected with HA-BMX, starved as in (E) and treated with DHEA for 2 hours; p-BMX was detected by western blot.

Other Achievement 2: BMX directly phosphorylates 3βHSD1 at Y344.

To investigate the role of BMX in phosphorylation of 3βHSD1, we inhibited BMX activity in C4-2 and LNCaP cells. Immunoblotting analyses of immunoprecipitated HA-3βHSD1 with anti-phospho-tyrosine and anti-3βHSD1 pY344 antibodies showed that the BMX inhibitors ibrutinib and zanubrutinib blocked DHEA-induced phosphorylation of 3βHSD1 (**Fig. 3, A to C**). We overexpressed HA-BMX in C4-2 and LNCaP cells. Immunoblotting analyses of immunoprecipitated HA-3βHSD1 with anti-3βHSD1 pY344 antibodies showed BMX enhanced phosphorylation of 3βHSD1 pY344 (**Fig. 3D**). Moreover, knockdown of BMX substantially reduced 3βHSD1 pY344 phosphorylation in LNCaP cells (**Fig. 3E**). Furthermore, overexpression of a kinase-dead BMX mutant (BMX-KD) in C4-2 cells strikingly failed to stimulate 3βHSD1 pY344 phosphorylation that, in contrast, was induced by WT-

BMX (**Fig. 3F**). To determine whether BMX directly phosphorylates 3βHSD1, we carried out *in vitro* kinase assays by mixing purified GST-3βHSD1 and HA-BMX. The assays showed that BMX directly phosphorylated 3βHSD1 at Y344 (**Fig. 3G**). These results indicate that BMX is the kinase that directly phosphorylates 3βHSD1 at Y344.

Other Achievement 3: 3βHSD1 pY344 enhances dimerization.

We next investigated how Y344 phosphorylation promotes 3βHSD1 cellular enzymatic activity. We purified 3βHSD1 or 3βHSD1-Y344F mutant and performed an NAD+ turnover assay *in vitro*. The results showed that WT enzyme purified from zanubrutinib-treated cells and the phospho-mutant of 3βHSD1 had lower catalytic activity (Kcat/Km); WT enzyme purified from cells with overexpressed BMX had a marginal increase in catalytic activity (Kcat/Km), and no significant increase in Kcat/Km was observed for 3βHSD1 phospho-mutant expressed in cells with overexpressed BMX (**Fig. 3, H and J**). 3βHSD1 phosphorylation did not significantly affect the Michaelis constant (Km) of DHEA (**Fig. 3I**). These results suggest that in a purified *in vitro* context, phosphorylation appears to have minimal influence on observed enzymatic activity. Furthermore, phosphorylation of Y344 at 3βHSD1 had no effect on its protein expression or degradation (**Fig. S3, A and C**), nor did zanubrutinib affect the level of 3βHSD1 protein expression (**Fig. S3B**). Some hydroxysteroid dehydrogenase enzymes are known to exist as dimers. To further investigate how Y344 phosphorylation may influence 3βHSD1 activity, we tested whether Y344 phosphorylation regulates 3βHSD1 dimer formation in C4-2 cells co-transfected with Flag-3βHSD1 and GST-3βHSD1 and treated with DHEA. Co-immunoprecipitation of Flag-3βHSD1 and GST-3βHSD1 was inhibited by blocking Y-phosphorylation using the Y344F mutation, as well as with zanubrutinib treatment, suggesting that 3βHSD1 pY344 enhances dimerization in cells (**Fig. 3, K and L**). These results suggest that phosphorylation may promote cellular dimerization and thus enhance enzymatic activity of 3βHSD1 in a cellular context.

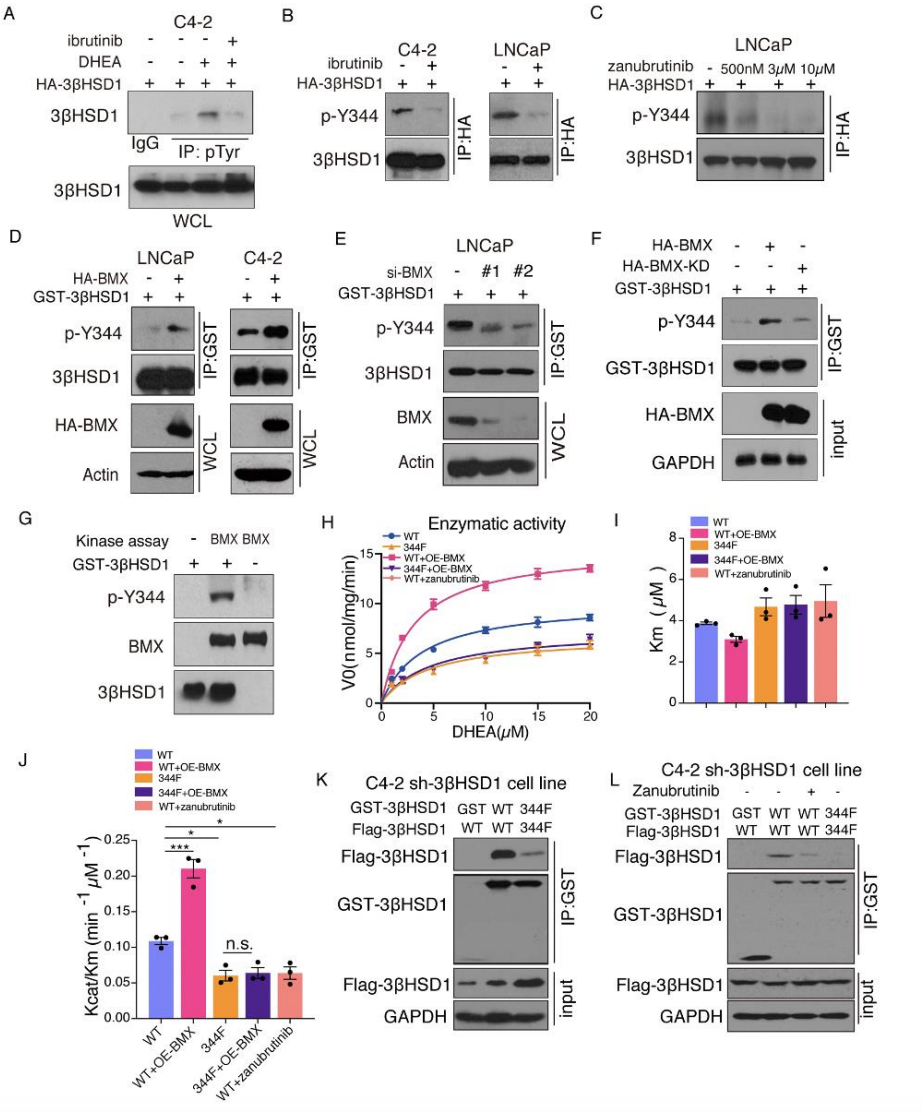

Fig 3. BMX directly binds 3βHSD1 and phosphorylates Y344. A. LNCaP cells overexpressing 3βHSD1 were treated with ibrutinib for 1.5 hours with or without DHEA for 0.5 hours. Pan-phospho-tyrosine (pTyr) was detected by immunoprecipitation and western blot. **B and C.** Cells overexpressing 3βHSD1 were treated with ibrutinib or zanubrutinib for 3 hours, and DHEA for 1 or 2 hours, respectively. Phospho-3βHSD1-Y344 was detected by immunoprecipitation and western blot. Blots run in parallel, contemporaneously, using identical samples are shown. **D.** Cells with co-overexpression of 3βHSD1-GST and HA-BMX or vehicle were treated with DHEA for 1 hour. Phospho-3βHSD1-Y344 was detected by immunoprecipitation and western blot. Actin blots, serving as loading controls, were run in parallel, contemporaneously using identical samples with other blots. **E.** Cells overexpressing 3βHSD1-GST were transfected with siNT or one of two siRNA sequences against BMX; phospho-3βHSD1-Y344 was detected by GST pull-down and western blot. 3βHSD1 blots, serving as loading controls, were run in parallel, contemporaneously using identical samples with other blots. **F.** Cells with co-overexpression of 3βHSD1-GST and HA-BMX or HA-BMX-KD (kinase dead) were treated with DHEA for 1 hour. Phospho-3βHSD1-Y344 was detected by immunoprecipitation and western blot. **G.** 3βHSD1-GST or HA-BMX was purified from 293T cells; 3βHSD1-GST was dephosphorylated using phosphatase in vitro, followed by a kinase assay and western blot. **H, I, J.** 293T cells were transfected with 3βHSD1 or Y344F mutant with or without co-overexpressed HA-BMX. 3βHSD1 or 3βHSD1-Y344F mutant was immunopurified, and an NAD+ turnover assay was performed. Mean ± SEM represents combined data from 3 independent experiments. *P < 0.05, *** P < 0.001 (1-way ANOVA with Bonferroni's multiple comparisons test). **K.** GST-tagged and flag-tagged WT or Y344F-3βHSD1 were transfected into C4-2 cells, GST pull-down was performed, and flag-tagged 3βHSD1 was detected by western blot. Cells were treated with DHEA for 2 hours. **L.** GST-tagged and flag-tagged WT or Y344F-3βHSD1 were transfected into C4-2 cells, GST pull-down was performed, and flag-tagged 3βHSD1 was detected by western blot. Cells were treated with DHEA for 2 hours; zanubrutinib (10 μM) treatment was 24 hours.

Other Achievement 4: BMX blockade and inhibition of 3βHSD1 phosphorylation impedes expression of androgen-regulated genes and prostate cancer proliferation.

To explore whether targeting regulatory kinases can inhibit prostate cancer cell proliferation, we generated LNCaP cells stably expressing shNT (non-targeting control) or two shRNA sequences against BMX. After overnight serum deprivation, we assessed proliferation in the presence or absence of DHEA. The results indicated that knocking down BMX inhibited cell proliferation that is induced by DHEA (**Fig. 4D**). In addition, qPCR results showed that knocking down BMX reduced DHEA-induced AR transcriptional activity (**Fig. 4E**). Based on these findings, we hypothesized that BMX inhibitors also inhibit prostate cancer proliferative activity. We treated LNCaP and C4-2 cells with zanubrutinib and determined cell proliferation and AR target gene expression. Our results demonstrated that zanubrutinib effectively inhibited proliferation (**Fig. 4F**) and AR transcriptional activity in the presence of DHEA (**Fig. 4G**) in LNCaP and C4-2 cells. We also treated LNCaP and C-42 cells with another BMX inhibitor, ibrutinib, and assessed viability using Trypan blue staining (**Fig. S4, A and B**), the results of which were consistent with the cell proliferation results. To further address the specificity of BMX inhibitors, we performed experiments with BMX overexpression in LNCaP and C4-2. The effects of BMX overexpression on 3βHSD1 phosphorylation, DHEA metabolism, AR signaling and cell proliferation are all reversible with BMX pharmacologic inhibition (**Fig. S4, C-F**). In conclusion, our findings suggest that the phosphorylation of 3βHSD1 Y344 promotes prostate cancer proliferation, and targeting BMX as its regulatory kinase blocks the growth of prostate cancer cells.

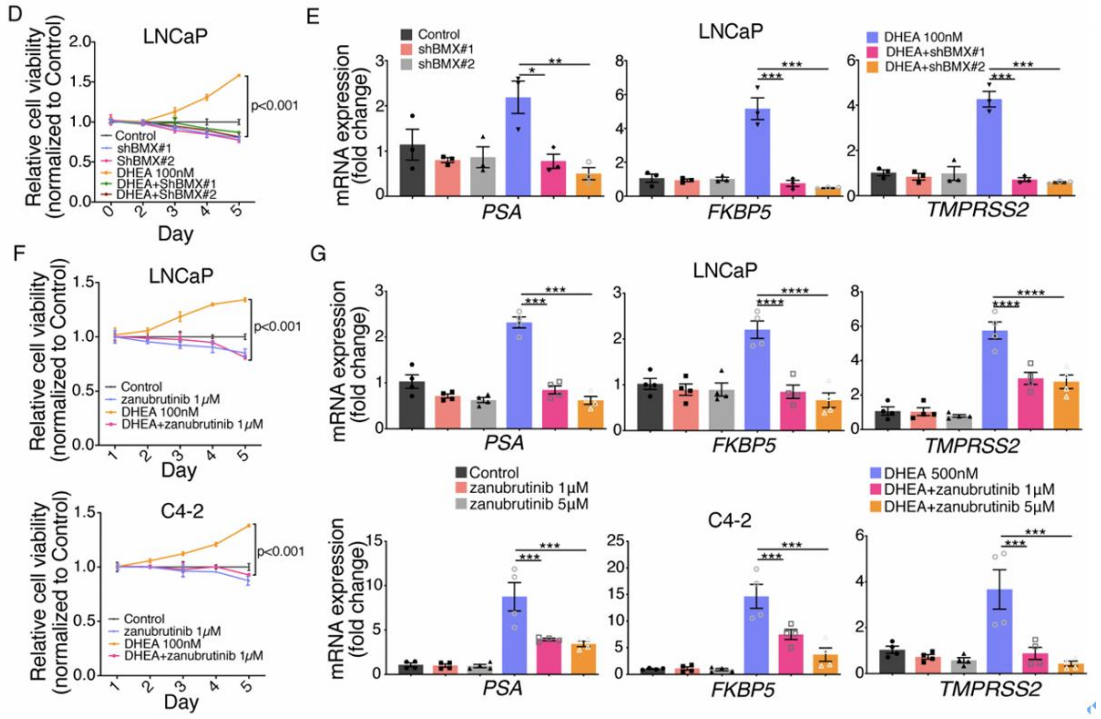

Fig 4. BMX blockade and inhibition of 3βHSD1 phosphorylation inhibit expression of androgen-regulated genes and prostate cancer proliferation. D. Cells stably expressing shNT or one of two shRNA sequences against BMX were deprived of serum overnight, followed by treatment with DHEA and cell proliferation assessment as in (B). **E.** As in (C), except that RNA extraction and qPCR was done on shBMX or control cells treated with DHEA for 48 hours. **F.** LNCaP or C4-2 cells were deprived of serum overnight, treated with zanubrutinib or DHEA for the indicated times, and cell proliferation assessed as in (B). **G.** LNCaP or C4-2 cells were deprived of serum overnight and treated with zanubrutinib or DHEA for 48 hours, followed by RNA extraction and qPCR. Expression is normalized to control and *RPLP0* expression. For (A) and (C), mean ± SEM represents combined data from 3 biological independent replicates performed in technical triplicate (unpaired 2-tailed t-test). For (B), (D), and (F), mean ± SEM represents 3 replicates in 1 experiment. Three independent experiments were performed (2-way ANOVA with Bonferroni's multiple comparisons test). For (E), mean ± SEM represents combined data from 3 biological independent replicates performed in technical triplicates (1-way ANOVA with Bonferroni's multiple comparisons test). For (G), mean ± SEM represents 4 replicates in 1 experiment. Three independent experiments were performed (1-way ANOVA with Bonferroni's multiple comparisons test). * P < 0.05, **P < 0.01, *** P < 0.001, **** P < 0.0001.

Other Achievement 5: Pharmacologic BMX blockade inhibits androgen biosynthesis and CRPC growth *in vivo*.

To investigate whether targeting phosphorylation blocks prostate cancer growth *in vivo*, we determined how effectively zanubrutinib blocked CRPC growth using mouse xenograft models. We established C4-2 or VCaP CRPC tumors with castration and DHEA pellet implantation. The mice were treated with zanubrutinib at a dose of 15 mg/kg or vehicle by oral gavage twice daily. Treatment with zanubrutinib led to significant tumor growth inhibition in both models compared to vehicle control (P < 0.0001) (**Fig. 5, E and J**). In contrast, zanubrutinib had virtually no effect on growth and androgen signaling in xenografts growing in eugonadal mice (**Fig. S5, E and J**). Differences in progression-free survival were similarly significant for zanubrutinib treatment in mice with CRPC (**Fig. 5, F and K**; P < 0.0001) but not xenografts grown in the eugonadal mice (**Fig. S5, F and K**). Tumors from zanubrutinib-treated mice with CRPC displayed lower androgen production and AR target gene (*PSA, FKBP5, TMPRSS2*) expression (**Fig. 5, G, H and L, M**). By contrast, zanubrutinib had no significant effect on untreated tumors (**Fig. S5, G, H and L, M**). Unbiased RNA-Seq and Gene Set Enrichment Analysis (GSEA) similarly demonstrated that zanubrutinib inhibited AR-regulated genes (**Fig. 5I**). Zanubrutinib had no significant effect on AR regulation in eugonadal tumors (**Fig. S5E**).

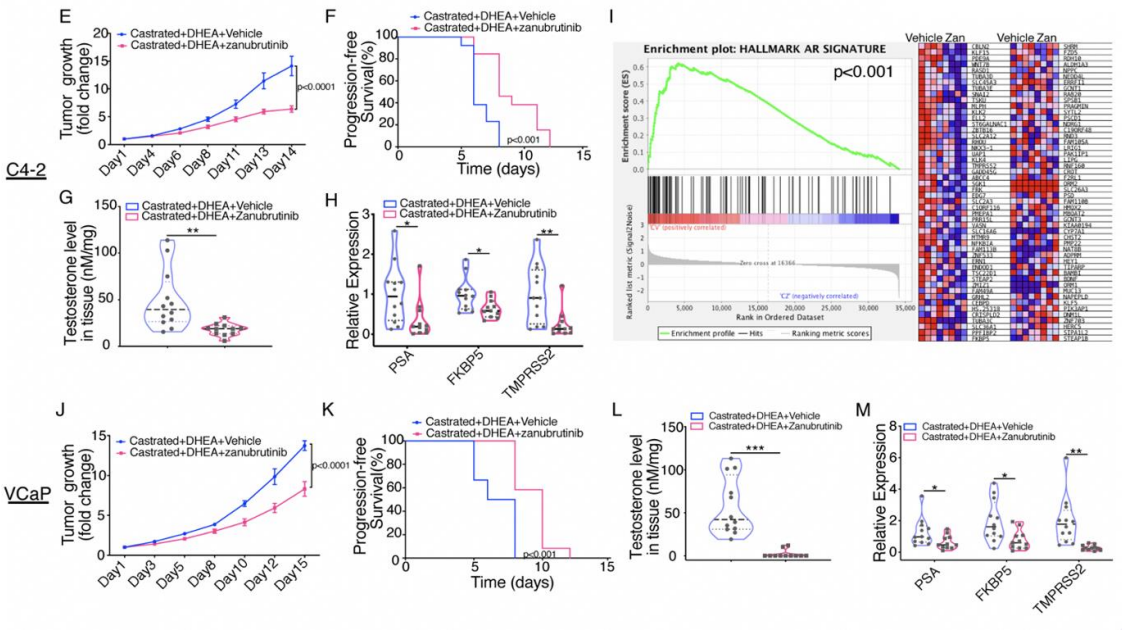

Fig 5. 3βHSD1-Y344F BMX pharmacologic blockade and 3βHSD1-Y344F inhibit androgen biosynthesis and CRPC growth in vivo. E. Six million C4-2 cells were injected subcutaneously in mice, and castration, DHEA pellet implantation, and treatment with vehicle or zanubrutinib at a dose of 15 mg/kg by oral gavage twice daily was performed after tumors reached 150 mm^3. Tumor growth was assessed as fold change from time of treatment initiation. The numbers of mice in the castration/vehicle and castration/zanubrutinib groups were 13 and 12, respectively. **F.** Progression-free survival was assessed as time to 3-fold increase in tumor volume from treatment initiation. **G.** Tumor testosterone in xenograft tumors was detected by mass spectrometry. **H.** Expression of AR-regulated genes was assessed by qPCR and expression is normalized to control and *RPLP0* as in (D). **I.** RNA-seq and gene set enrichment analysis was performed, showing AR inhibition as the top upstream regulator predicted as inhibited. **J.** Ten million VCaP cells were injected subcutaneously. Castration, DHEA pellet implantation, and vehicle or zanubrutinib at a dose of 15 mg/kg by oral gavage twice daily were performed after tumors reached 200 mm^3, and fold-change in tumor volume from the time of treatment initiation was assessed. The numbers of mice in the castration/vehicle and castration/zanubrutinib groups were 12 and 11, respectively. **K.** Progression-free survival was assessed as in (B). **L.** Xenograft testosterone detection by mass spectrometry. **M.** AR-regulated genes were assessed as in (D).

Other Achievement 6: Effects of BMX inhibition on 3βHSD phosphorylation and androgen synthesis in fresh human prostate tissues.

I next investigated the effects of BMX pharmacologic blockade in fresh prostate tissues cultured for metabolic assessment from men undergoing radical prostatectomy. Tissues were treated with [^{3}H]-DHEA with or without zanubrutinib, and HPLC was performed on steroids extracted from medium to detect metabolism to steroids downstream of 3βHSD1. Tissues from a total of 7 patients, all of whom harbored the adrenal-permissive *HSD3B1* allele (3 homozygous and 4 heterozygous) had detectable DHEA metabolism and thus were assessable for reversibility with zanubrutinib. Notably, our results showed that zanubrutinib inhibited DHEA metabolism in all 7 prostate tissues (**Fig. 6, A, B and Fig. S6**). Immunoprecipitation and western blot results showed that phosphorylation of 3βHSD1 was reduced by inhibiting BMX with zanubrutinib (**Fig. 6C**). In addition, the interaction between BMX and 3βHSD1 was observed in human prostate tissues (**Fig. 6D**). Taken together, these results show the potential therapeutic effects of targeting 3βHSD1 phosphorylation using BMX inhibitors for the treatment of men with CRPC (**Fig. 6E**) and more generally, the role of BMX in physiologic regulation of extragonadal sex steroid biosynthesis.

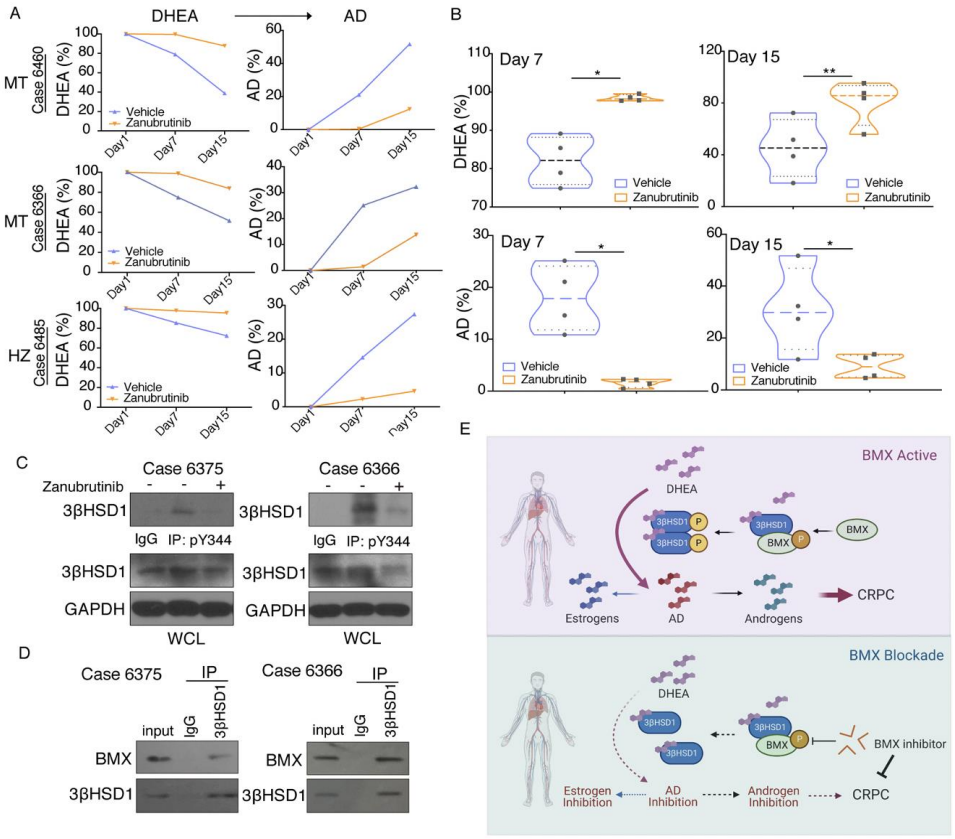

Fig 6. Targeting BMX inhibits phosphorylation and enzymatic activity of 3βHSD1 in prostate tissue of prostate cancer patients. A. Fresh prostate tissues from 3 representative patients with prostate cancer from a total of 7 patients in whom DHEA metabolism was detectable; DHEA metabolism was analyzed in a total of 42 patients (MT, homozygous *HSD3B1*(1245C); HZ, heterozygous). Tissues were obtained and aliquoted in two equal portions. One portion was treated with zanubrutinib and the other with DMSO. Both portions were maintained in 3 ml DMEM containing 10% fetal bovine serum, incubated for 12 hours, and then [^{3}H]-DHEA was added to each portion. Cell culture medium was collected at the indicated times, and HPLC was performed. **B.** DHEA metabolism was analyzed on day 7 and day 15. Mean ± SEM represents DHEA metabolism from 4 patients. * $P < 0.05$, **$P < 0.01$ (unpaired 2-tailed t-test). **C.** Protein was extracted from about 20 mg patient tissue, followed by 3βHSD1 immunoprecipitation and western blot. **D.** The remaining tissue was used for western blot: tissue cores were minced and aliquoted in 2 equal parts and treated as in (A). After 12 hours of culture, DHEA (10 nM) was added to each portion. Seven days later, protein was collected, and immunoprecipitation and western blot were performed. **E.** Proposed model for 3βHSD1 phosphorylation. BMX phosphorylates 3βHSD1 Y344 upon substrate activation Y344 phosphorylation enhances 3βHSD1 activity by increasing its dimerization, which subsequently promotes androgen production and prostate cancer proliferation. When BMX is inhibited, 3βHSD1-phosphorylation-stimulated dimerization is lost, reducing cellular enzyme activity, potent androgen production, and prostate cancer proliferation. For all panels, error bars represent the SEM; *P* values were calculated using paired two-tailed t tests.

Overall, the mechanisms and *in vivo* studies provide an entirely new strategy for the treatment of prostate cancer. Our data are serving as the basis for a multi-institutional phase 2 clinical trial of BMX inhibition in prostate cancer that will be initiated through the MSKCC DOD clinical trials consortium (FDA IND pending).

What opportunities for training and professional development has the project provided?

1. Attended Responsible Conduct of Research and Human Subjects training.
2. Attended monthly Prostate Cancer Working Group and Seminar Series
3. Attended and presented research at the weekly lab meetings and journal clubs
4. Attended and presented work at the weekly CCF Department of Cancer Biology seminars
5. Attend workshop “Biomedical and Scientific Writing” held by the Kenyon Institute, Kenyon Ohio.

How were the results disseminated to communities of interest?

1. My findings were published in the Journal of Clinical Investigation in 2022.
2. Submitted abstract to the American Association for Cancer Research Special Conference: Advances in Prostate Cancer Research, to be held March 15-18, 2023.

What do you plan to do during the next reporting period to accomplish the goals?

I plan to pursue aim 2 in the future.

IMPACT:

What was the impact on the development of the principal discipline(s) of the project?

If there is nothing significant to report during this reporting period, state "Nothing to Report."

The mechanisms and in vivo studies in our manuscript provide an entirely new strategy for the treatment of prostate cancer. Our data serve as the basis for a multi-institutional phase 2 clinical trial of BMX inhibition that will be initiated through the MSKCC DOD clinical trials consortium (FDA IND pending). Furthermore, emerging data on the missense-encoding HSD3B1 in breast cancer suggest that BMX inhibition may also play a role in the treatment of postmenopausal breast cancer.

What was the impact on other disciplines?

Nothing to Report

What was the impact on technology transfer?

Based on my mechanistic findings here, a multi-institutional phase 2 clinical trial of abivertinib plus abiraterone is underway for men with metastatic CRPC who inherit the adrenal-permissive HSD3B1 allele (NCT05361915). This trial is poised to test an entirely new mechanistic concept for the treatment of metastatic CRPC, in a disease and treatment space where use of kinase inhibitors have not previously been shown to be effective.

What was the impact on society beyond science and technology?

Based on my mechanistic findings here, a multi-institutional phase 2 clinical trial of abivertinib plus abiraterone is underway for men with metastatic CRPC who inherit the adrenal-permissive HSD3B1 allele (NCT05361915). This trial is poised to test an entirely new mechanistic concept for the treatment of metastatic CRPC, in a disease and treatment space where use of kinase inhibitors have not previously been shown to be effective.

CHANGES/PROBLEMS:

Changes in approach and reasons for change

When I mutated phosphorylated amino acids, only a single residue at tyrosine 344 appeared to be required for enzyme activity. Therefore, the other residues and kinases phosphorylating other amino acids were not pursued. However, there was no change in approach.

Actual or anticipated problems or delays and actions or plans to resolve them

Nothing to Report

Changes that had a significant impact on expenditures

Nothing to Report

Significant changes in use or care of human subjects, vertebrate animals, biohazards, and/or select agents

Nothing to Report

Significant changes in use or care of human subjects

Nothing to Report

Significant changes in use or care of vertebrate animals.

Nothing to Report

Significant changes in use of biohazards and/or select agents

Nothing to Report

PRODUCTS:

Publications, conference papers, and presentations

Journal publications.

My work was accepted in October 2022 and published by the *Journal of Clinical Investigation:*

Xiuxiu Li, Michael Berk, Christopher Goins, Mohammad Alyamani, Yoon-Mi Chung, Chenyao Wang, Monaben Patel, Nityam Rathi, Ziqi Zhu, Belinda Willard, Shaun Stauffer, Eric Klein, Nima Sharifi. BMX controls 3βHSD1 and sex steroid biosynthesis in cancer. J Clin Invest. 2023 Jan 17;133(2):e163498. doi: 10.1172/JCI163498. PMID: 36647826

Books or other non-periodical, one-time publications.

Nothing to Report

Other publications, conference papers, and presentations.

Nothing to Report

Website(s) or other Internet site(s)

Nothing to Report

Technologies or techniques

Nothing to Report

Inventions, patent applications, and/or licenses

Nothing to Report

Other Products

Nothing to Report

PARTICIPANTS & OTHER COLLABORATING ORGANIZATIONS

What individuals have worked on the project?

Name:	*Xiuxiu Li*
Project Role:	*Principal investigator*
Researcher Identifier (e.g.	*0000-0002-4106-318*

ORCID ID):	
Nearest person month worked:	*24*
Contribution to Project:	*Xiuxiu Li is responsible for designing, performing and interpreting the experiments and manuscript preparation.*
Funding Support:	

Has there been a change in the active other support of the PD/PI(s) or senior/key personnel since the last reporting period?

No Change.

What other organizations were involved as partners?

Nothing to Report.

SPECIAL REPORTING REQUIREMENTS

COLLABORATIVE AWARDS:

Nothing to Report.

QUAD CHARTS:

Nothing to Report.

APPENDICES:

Figures.

Supplementary Figures

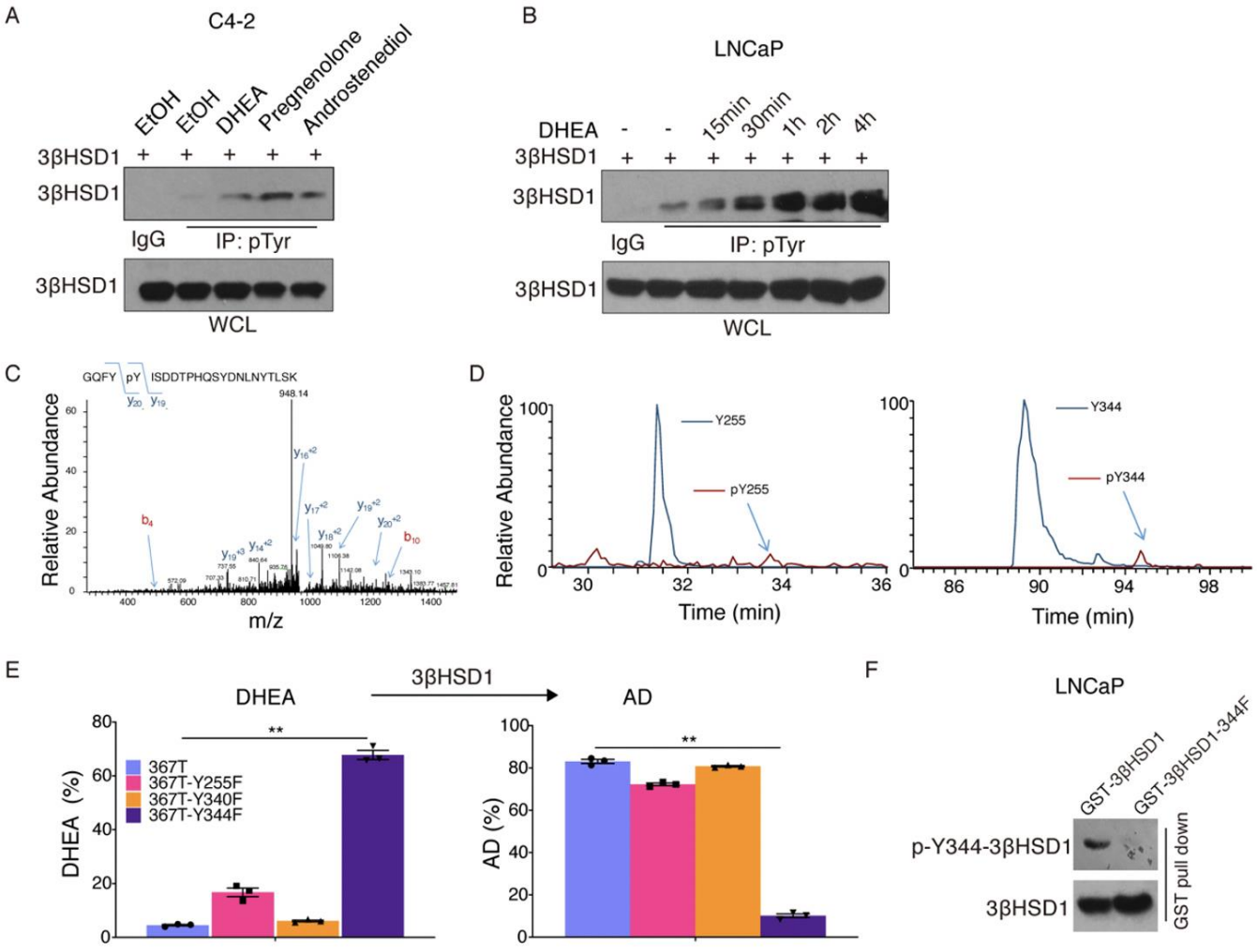

Supplemental Fig. 1. 3βHSD1 phosphorylation. A. C4-2 cells overexpressing HA-3βHSD1 were treated with the indicated steroids (10 nM) for 1 hour. Pan-phospho-tyrosine (pTyr) was detected by immunoprecipitation and western blot. **B.** LNCaP cells overexpressing HA-3βHSD1 were treated with DHEA (10 nM) for the indicated times. Pan-phospho-tyrosine (pTyr) was detected by immunoprecipitation and western blot. Lysate from cells expressing HA-3βHSD1 and no DHEA treatment were used for the IgG control. **C.** 3βHSD1-GST was transfected in C4-2 cells, and cells were treated with DHEA for 1 hour. GST pull-down complexes were immunoblotted, and the indicated phosphopeptides on human 3βHSD1 were identified by LC-MS/MS. A triply charged peptide with a mass of 983.75 Da was identified in a targeted analysis of GST-HSD3B1. The CID spectra for this peptide are dominated by doubly charged C-terminal y ions. The mass difference between y_{19} and y_{20} is consistent with modification at Y255. **D.** Chromatograms for the unmodified, Y255, and pY255 peptides from GST-HSD3B1 are shown as are chromatograms for the unmodified, Y344, and pY344 peptides from GST-HSD3B1. **E.** HA-3βHSD1 enzyme activity was assessed by determining DHEA metabolism with HPLC. Cells were transfected with HA-3βHSD1 mutants and subsequently treated with [^{3}H]-DHEA for 6 hours, followed by steroid extraction from media and steroid separation and quantitation with HPLC. Mean ± SEM represents 3 replicates in 1 experiment. Three independent experiments were performed. **P < 0.01 (1-way ANOVA test with Dunnett's multiple comparisons test). **F.** Validation of phospho-3βHSD1-Y344 antibody.

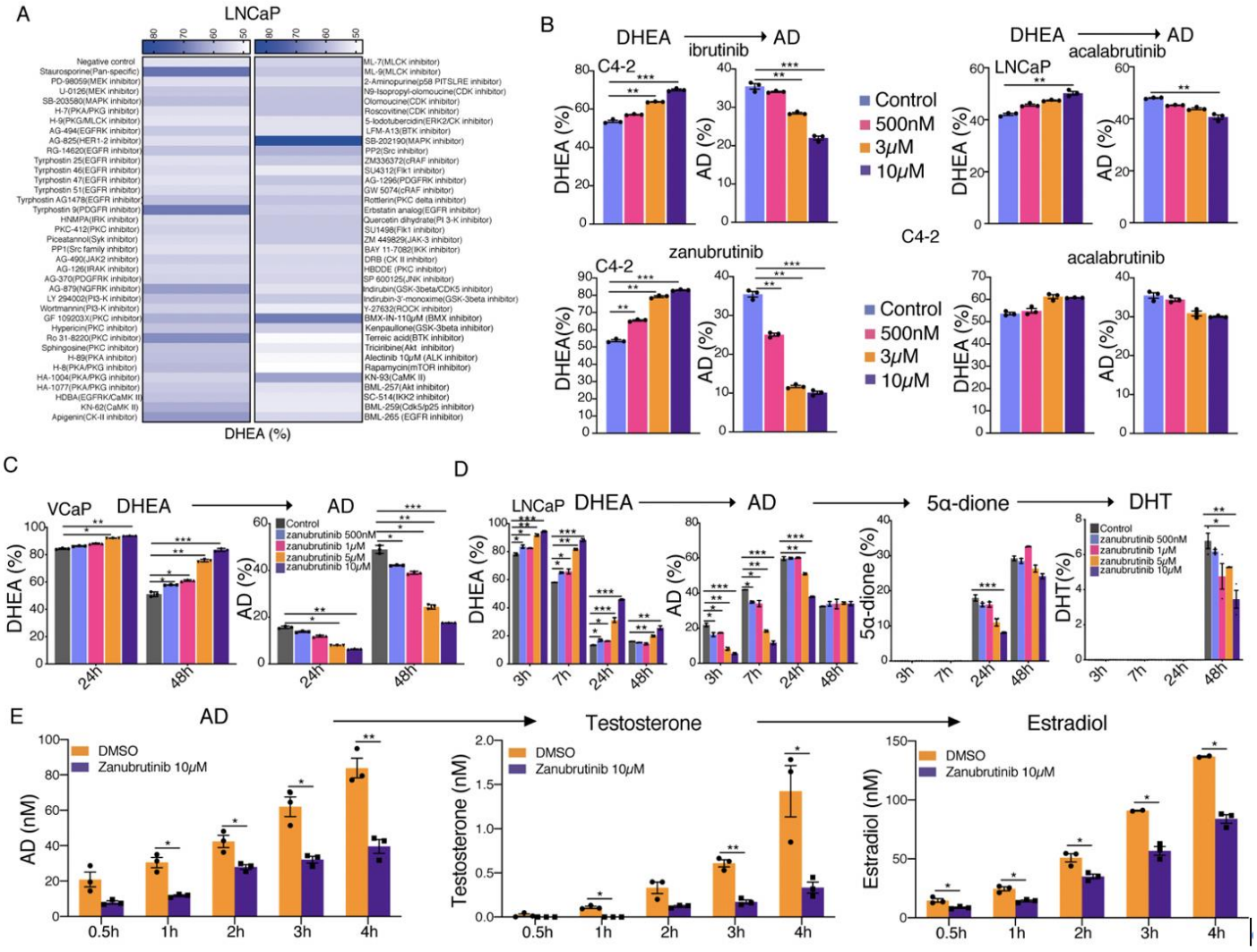

Supplemental Fig. 2. Tyrosine kinase inhibition and regulation of cellular 3βHSD1 activity. A. BMX inhibition suppresses DHEA metabolism. Kinase screening was performed by detecting DHEA metabolism using a kinase inhibitor library. LNCaP cells were treated with about 88 kinase inhibitors (10 μM) for 1 hour and subsequently treated with [^{3}H]-DHEA for 5 hours. Medium was then collected, and steroids were extracted and separated and quantified with HPLC. Color scale indicates % DHEA remaining. **B.** LNCaP or C4-2 cells were treated with BMX inhibitors for 1 hour and subsequently treated with [^{3}H]-DHEA for 5 hours. Medium was then collected and steroids were extracted from medium and separated and quantified with HPLC. **C, D.** As in (B), but experiments were done in both LNCaP and VCaP cell lines using various concentrations of zanubrutinib for the indicated times to determine effects on DHEA metabolism. **E.** JEG3 cells were starved with RPMI-1640 medium containing 10% charcoal-stripped fetal bovine serum; 24 hours later, 10 μM zanubrutinib was added, followed by DHEA 16 hours later. After DHEA addition, cells were cultured for the indicated times, medium was collected, and mass spectrometry was performed to detect the steroid level. For B, mean ± SEM represents 3 replicates in 1 experiment. Three independent experiments were performed (1-way ANOVA test with Dunnett's multiple comparisons test). For C and D, mean ± SEM represents combined data from 3 biological independent replicates performed in technical triplicate (1-way ANOVA test with Dunnett's multiple comparisons test). For E, mean ± SEM represents 3 replicates in 1 experiment. Three independent experiments were performed (multiple unpaired t-tests). * P < 0.05, **P < 0.01, *** P < 0.001, **** P < 0.0001.

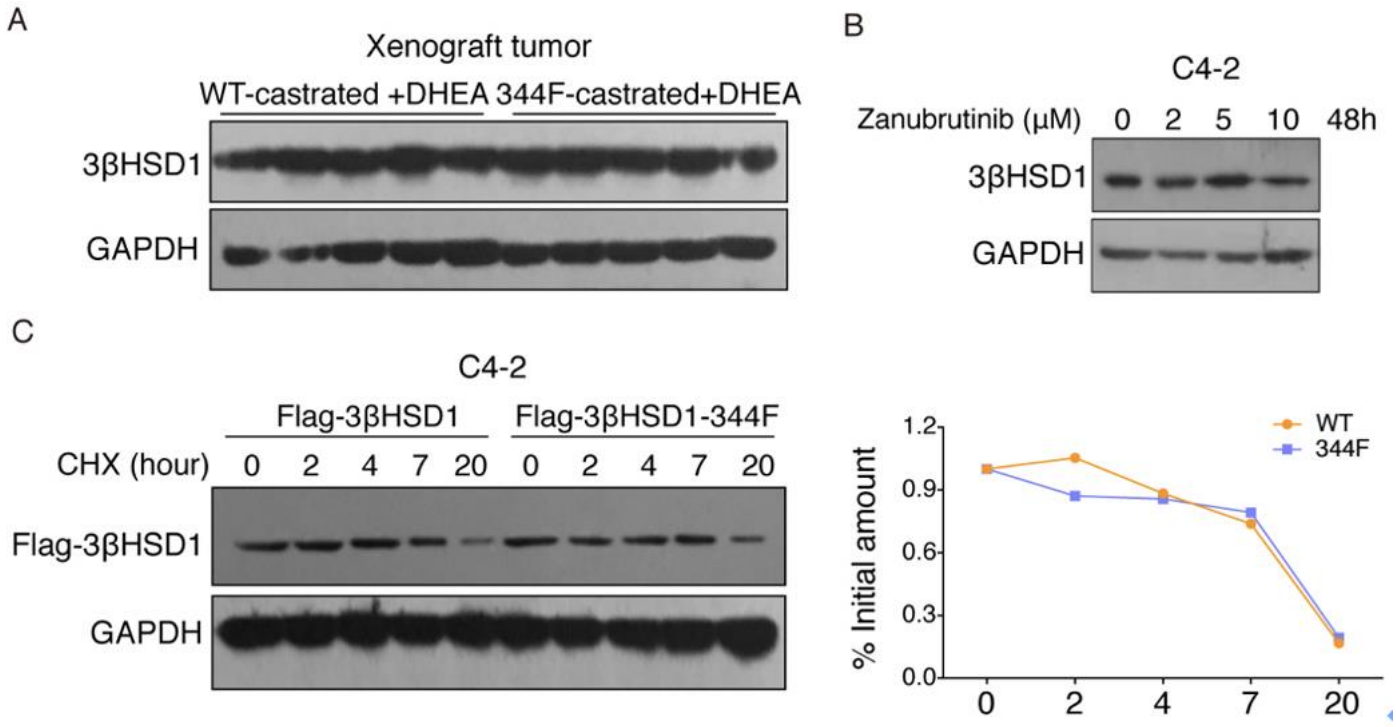

Supplemental Fig. 3. Effects of 3βHSD1-Y344F mutation on protein levels. A. C4-2 cells with stable shRNA-mediated knockdown of 3βHSD1 were stably infected with a lentivirus expressing 3βHSD1 (WT) or 3βHSD1-Y344F grown in castrated mice after tumors reached 200 mm^3. Proteins were extracted from tumor tissue, and western blot was performed. **B.** C4-2 cells were treated with 2, 5, or 10 μM zanubrutinib for 48 hours. Proteins were extracted, and western blot was performed. Blots run in parallel, contemporaneously, using identical samples are shown. **C.** Flag-tagged WT or Y344F-3βHSD1 was transfected into C4-2 cells; then cells were treated with cyclohexamide (CHX) for the indicated times, followed by protein extraction, western blot, and protein quantitation.

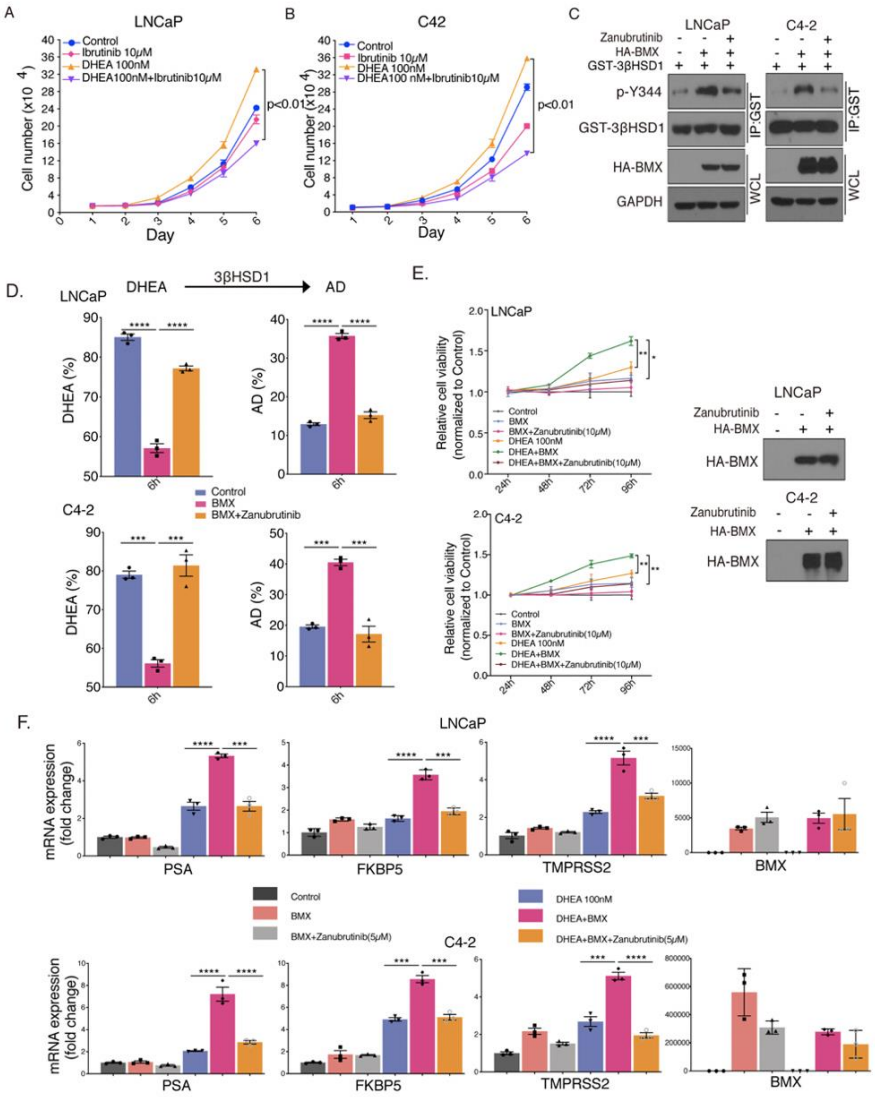

Supplemental Fig. 4. Effects of BMX inhibition on cell viability. A. LNCaP cells were deprived of serum overnight, followed by treatment with ibrutinib or DHEA for the indicated times, and the number of viable cells was determined by Trypan blue exclusion assay. **B.** C4-2 cells were deprived of serum overnight, followed by treatment with ibrutinib or DHEA for the indicated times, and the viable cell number was determined with Trypan blue. **C.** Cells overexpressing 3βHSD1 or BMX were treated with zanubrutinib for 3 hours, and DHEA for 1 or 2 hours, respectively. Phospho-3βHSD1-Y344 was detected by immunoprecipitation and western blot. 3BHSD1(T) and GAPDH blots serving as loading controls, were run in parallel, contemporaneously using identical samples with other blots. **D.** Cells overexpressing BMX were treated with zanubrutinib for 3 hours and subsequently treated with [^{3}H]-DHEA for 6 hours, followed by steroid extraction from media and steroid separation and quantitation with HPLC. **E.** As in (D), but cells were deprived of serum overnight, followed by treatment with DHEA for the indicated days; cell proliferation was assessed with the WST-1 assay, and growth for each cell line was normalized to WT control for each designated day. Proteins were lysed for 96 hours, then cells were collected and western blot was performed to detect the effect of BMX overexpression. **F.** As in (D), but cells were deprived of serum overnight and treated with DHEA for 48 hours, followed by RNA extraction and qPCR. Expression is normalized to control and *RPLP0* expression. For A and B, mean ± SEM represents combined data from 3 biological replicates performed in technical triplicate (2-way ANOVA test with Bonferroni's multiple comparisons test). For D and F, mean ± SEM represents 3 replicates in 1 experiment. Three independent experiments were performed (1-way ANOVA test with Bonferroni's multiple comparisons test). For E, mean ± SEM represents combined data from 3 biological replicates performed in technical triplicate (2-way ANOVA test with Tukey's multiple comparisons test).

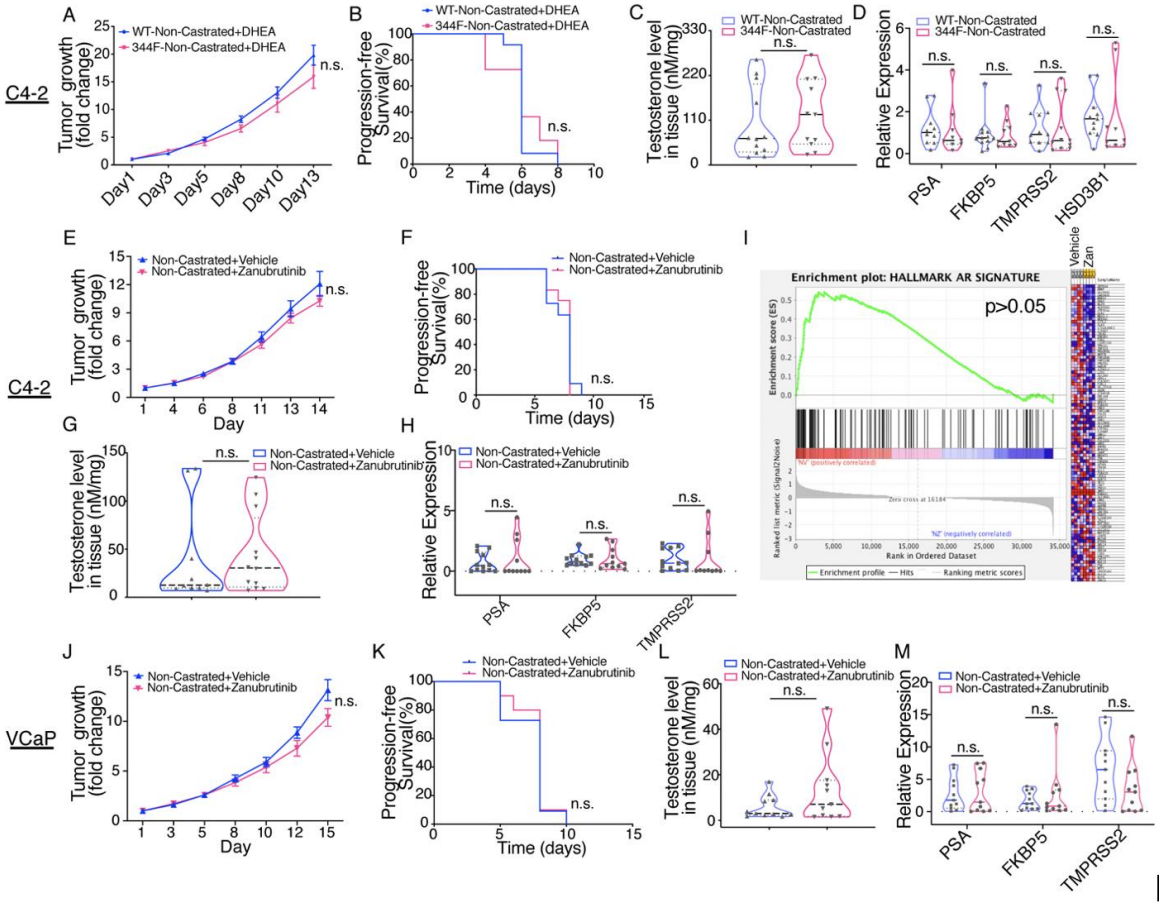

Supplemental Fig. 5. The effect of pharmacologic BMX inhibition and 3βHSD1-Y344F on xenografts in eugonadal mice. A. C4-2 cells with stable shRNA-mediated knockdown of 3βHSD1 were stably infected with a lentivirus expressing 3βHSD1 (WT) or 3βHSD1-Y344F. Mice were subcutaneously injected with 10 million cells. Tumor growth is shown as fold change from the time when tumors reached 200 mm^3. The numbers of mice in the WT-3βHSD1/eugondal and 344F-3βHSD1/eugonadal groups were 12 and 11, respectively. **B.** Progression-free survival was assessed as time to 3-fold increase in tumor volume from the time tumors reached 200 mm^3. **C.** Testosterone concentration in xenograft tumors was detected by mass spectrometry. **D.** RNA was extracted from xenograft tumors and gene expression was determined by qPCR. **E.** Six million C4-2 cells were injected subcutaneously in mice. After tumors reached 150 mm^3, zanubrutinib or vehicle treatment was started. Tumor growth was analyzed. The numbers of mice in the eugonadal/vehicle and eugonadal/zanubrutinib groups were 11 and 12 respectively. **F.** progression-free survival was assessed as time to 3-fold increase in tumor volume from treatment initiation. **G.** Absolute concentration of testosterone in xenograft tumors was detected by mass spectrometry. **H.** RNA was extracted from xenograft tumors, and AR target gene expression was determined by qPCR. Expression is normalized to control and *RPLP0* expression. **I.** RNA-seq was performed with 4 tumors from each group and Gene Set Enrichment Analysis was done for the AR signature gene set. **J.** Ten million VCaP cells were injected subcutaneously in mice, and treatment with vehicle or zanubrutinib was initiated when tumor volume reached 200 mm^3. There were 11 mice in each cohort for the eugonadal/vehicle and eugonadal/zanubrutinib groups. **K.** Progression-free survival was assessed as time to 3-fold increase in tumor volume from treatment initiation, and the significance of the difference between groups was calculated with a log-rank test. **L.** Testosterone in xenograft tumors was detected by mass spectrometry. **M.** AR target gene expression was determined as in (H). For A,E, and J, *P* values were calculated with 2-way ANOVA test with Bonferroni's multiple comparisons test. For B.F.K. *P* values were calculated with a log-rank test. For C, D, G, H, L, and M, *P* values were calculated using an unpaired 2-tailed t-test. n.s, no significant difference.

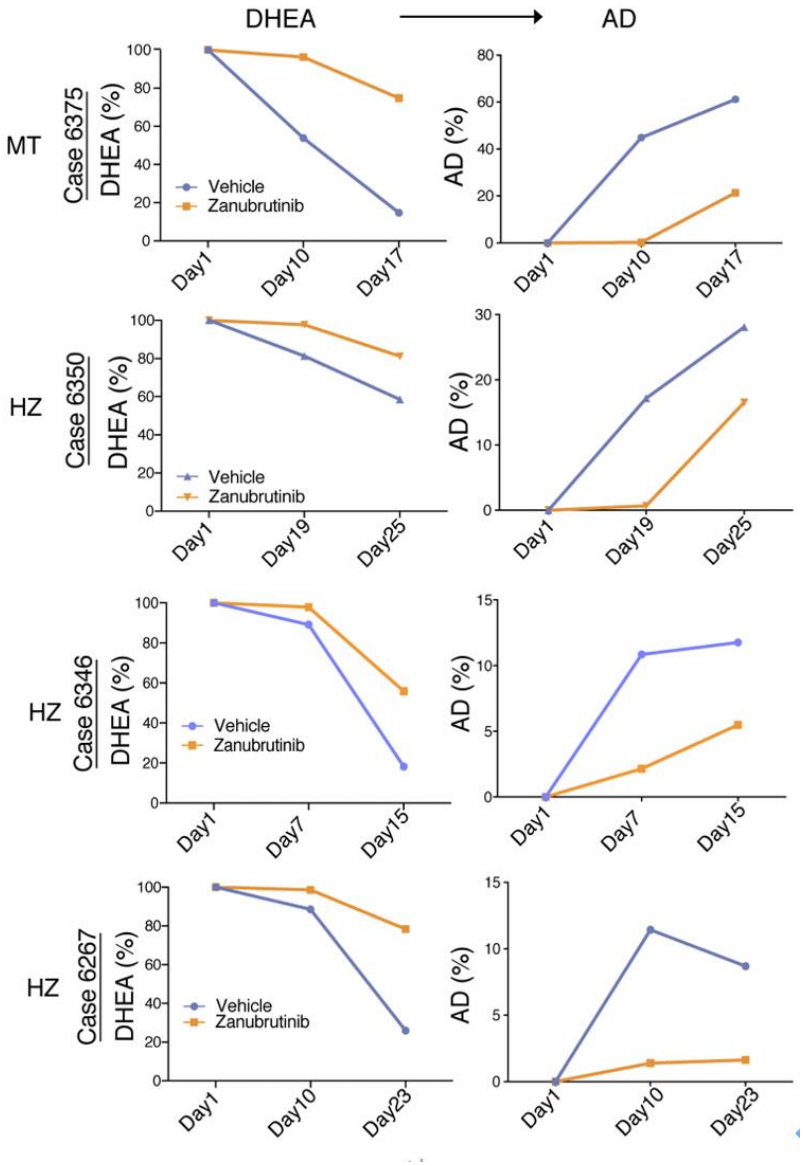

Supplemental Fig. 6. Effects of zanubrutinib on 3βHSD1 activity in human prostate tissue.
Fresh prostate tissue cores (40 - 60 mg) from 4 patients were obtained, minced, and aliquoted in two equal portions. One was treated with zanubrutinib, and the other was treated with DMSO. Both tissues were maintained in 3 mL DMEM containing 10% fetal bovine serum and incubated in a 5% CO_2 humidified incubator. After 12 hours of culture, [^{3}H]-DHEA was added to each portion. Cell culture medium was collected, and HPLC was performed.